ELSEVIER

Polymer 41 (2000) 5339–5348

polymer

Coherence of thermal transitions in poly(*N*-vinyl pyrrolidone)–poly(ethylene glycol) compatible blends 2. The temperature of maximum cold crystallization rate versus glass transition

M.M. Feldstein*, S.A. Kuptsov, G.A. Shandryuk

A.V. Topchiev Institute for Petrochemical Synthesis, Russian Academy of Sciences, 29 Leninsky prospekt, 117912, Moscow, Russian Federation

Received 3 August 1999; accepted 8 September 1999

Abstract

Differential scanning calorimeteric (DSC) heating thermograms of amorphous poly(*N*-vinyl pyrollidone) (PVP) blends with short-chain poly(ethylene glycol) (PEG) feature exotherms of cold crystallization coupled with symmetric melting endotherms, which relate to the state of the crystalline component, PEG, while PVP–PEG hydrogen-bonded complex reveals itself as an amorphous phase. As PEG content in blends exceeds a characteristic level, PEG cold crystallization occurs upon heating of the cool-quenched samples through their glass transition temperatures (T_g). The contributions of both thermodynamic and kinetic factors to the occurrence of non-crystallizable PEG have been analysed by considering the dependence of the PEG cold crystallization temperature, T_c, on blend T_g and composition along with the compositional dependence of the heat of melting of PEG. The stoichiometry of the PVP–PEG H-complex was evaluated from DSC thermograms as the amount of non-crystallizable PEG in PVP-underloaded blends. © 2000 Elsevier Science Ltd. All rights reserved.

Keywords: Relationship between the temperatures of cold crystallization and glass transition; State of poly(ethylene glycol); Stoichiometry of poly(*N*-vinyl pyrrolidone)–poly(ethylene glycol) hydrogen-bonded complex

1. Introduction

Recently, considerable attention has been focused on the preparation and examination of crystalline–amorphous compatible polymer blends [1–13], and currently all the studied crystalline–amorphous polymer mixtures are shown to share three general characteristics. Firstly, the two polymers are thought to be compatible and miscible in the molten state. Secondly, as the blends are cooled from the melt, crystallization of the crystallizable component occurs, but the total degree of crystallinity of the blends, determined from the area of the melting endotherm (ΔH_m), decreases rapidly with increasing content of the amorphous component. As the result of such behaviour, crystallization is inhibited below some critical concentration of the crystallizable polymer and no level of crystallinity is detected in blends containing an excess of the amorphous polymer. A third characteristic feature of the crystalline–amorphous blends is a substantial depression of melting temperature, T_m, resulting from the diluent effect of the amorphous component [1].

Over the past years progress has been made primarily on the impact of the amorphous polymer upon the melting point behaviour of the crystalline component, providing an insight into the thermodynamics of polymer interaction [1–3,5–12]. At the same time, few studies have been concerned with the amorphous polymer diluent's effect on blend crystallinity [1,4,13]. Meanwhile a question is pertinent: is the presence of non-crystallizable fraction of crystalline polymer due to specific interaction (binding) with the amorphous component, which is reported to be prerequisite for polymer compatibility [1], or is it a consequence of kinetic hindrance imposed by amorphous polymer upon crystallization process. Evidently, the kinetic effects can be caused by conventional dilution of crystalline polymer with amorphous component and the occurrence of specific interaction between polymers enhances these effects. Deconvolution of the thermodynamic and kinetic factors affecting melting behaviour of favourably interacting polymer blends provides the determination of interpolymeric binding degree based on differential scanning calorimetric (DSC) analysis of the composition dependence of melting

* Corresponding author. Fax: +7-095-230-2224.
E-mail address: mfeld@ips.ac.ru (M.M. Feldstein).

0032-3861/00/$ - see front matter © 2000 Elsevier Science Ltd. All rights reserved.
PII: S0032-3861(99)00688-6

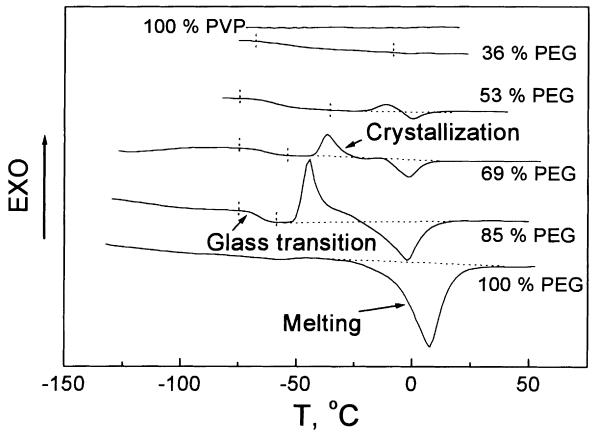

Fig. 1. Differential scanning calorimeter heating traces of PVP, PEG-400 and their freshly-prepared blends, covering entire composition range (in wt% of PEG).

endotherm area. With this purpose, the kinetic contribution to blend crystallinity must be closely examined in DSC traces. This necessitates the study of blend crystallization in conjunction with compositional behaviour of the glass transition temperature, T_g, and heat of fusion of crystalline polymer, ΔH_m.

In a recent paper [14], we have described the phase behaviour of poly(*N*-vinyl pyrrolidone) (PVP) compatible blends with a low molecular fraction of poly(ethylene glycol) (PEG) of $M_w = 400\ g\ mol^{-1}$. PVP is an amorphous polymer with $T_g = 178°C$, whereas crystalline PEG-400 ($T_m = 6°C$, $\Delta H_m = 118.4\ J\ g^{-1}$) at ambient temperature is in a molten, liquid state ($T_g = -70°C$). Owing to large negative deviations from a simple rule of mixing, observed in compositional behaviour of PVP–PEG blend T_g, all the blends considered in this study display $T_g < -40°C$. At room temperature they are in the viscoelastic state.

The PVP–PEG compatibility is due to complex formation through hydrogen bonding of hydroxyl groups at the ends of comparatively short PEG chains to the carbonyls in the repeat units of longer PVP macromolecules [15]. The invariability of PVP–PEG binding degree over a wide range of blend compositions reveals the stoichiometry of the hydrogen-bonded complex. In this complex, per every 100 PVP repeat units available in blend, no more than 27 PEG macromolecules, bearing together 54 terminal hydroxyl groups, have been shown to form H-bonds with 54 PVP units, while the other 46 units remain intact [16]. PVP–PEG binding degree was measured from the FT-IR spectra of blends in carbonyl and hydroxyl stretching vibration regions [17], and assessed also from DSC data using the observed composition dependence of blend T_g [18]. Both methods were found to give similar results [16]. Expressed in the terms of PEG weight fraction in blends, w_{PEG}, the stoichiometric composition of the PVP–PEG complex corresponds to $w_{PEG} \approx 0.36$. Even in comparatively dilute, 15% PVP solution in liquid PEG-400, only 56% of the PVP units form H-bonds with PEG hydroxyls, including 25–30% of tightly bound PVP units. The remaining 44% of the PVP units are not involved in the complexation in dilute solution, since a heat of hydrogen bonding for these units is thought to cease to dominant the negative change in PVP–PEG interaction entropy associated with ordered complex structure formation.

In the first of this series of papers [14] we presented results demonstrating the coherent phase behaviour of compatible PVP–PEG blends. As the blends were quench-cooled from the melt to $-100°C$ and then heated up through T_g with a rate of $20°C\ min^{-1}$, the following thermal events were observed: (1) a single, composition-dependent glass transition (T_g), approaching with decreasing PVP content the value found for pure PEG-400; (2) an exotherm of free PEG cold crystallization in couple with an endotherm of PEG melting; and (3) an endotherm corresponding to moisture desorption at $T > 100°C$. Numerical correlations were obtained from DSC traces among T_g, the temperature of PEG melting (T_m) and the temperature of free PEG maximum cold crystallization rate (T_c). The latter temperature corresponds to the maximum of the cold crystallization endotherm in heating scans. Inference drawn from these correlations implies an activation energy as a factor controlling the interrelationships between T_g, T_m and T_c [19].

The present research complements the foregoing work [14] by refining our insight into the mechanism of T_c–T_g dependence under heating quench-cooled melts of crystalline-amorphous polymer blends, and by including into consideration the thermodynamic factors embedded in the heat of fusion of crystalline polymer, ΔH_m. Since T_g reflects fundamental properties of compatible blends and characterises the amorphous phase, while T_c and ΔH_m are mainly associated with the state of the crystalline component in blend, the present approach is also thought to enable us to expand our comprehension of the state of PEG in the blends containing amorphous polymer.

2. Experimental

PVP (Kollidon K-90), $M_w = 1\ 000\ 000\ g\ mol^{-1}$ and PEG-400 (Lutrol E-400), $M_w = 400\ g\ mol^{-1}$, were obtained from BASF. PEG of molecular weight of $1000\ g\ mol^{-1}$ (PEG-1000) was produced by Fluka. All polymers were used as received.

The basic experimental procedures employed in this work were introduced in previous paper in this series [14]. The PVP–PEG blends, spanning the entire range of compositions, were prepared by drying the polymer component solutions in common solvent (ethyl alcohol). So-called “fresh” or “hydrated” blends were obtained by drying the solutions at ambient temperature and contained 7.2 ± 2.2 wt%. residual water, whereas “dry” blends were produced by drying the hydrated (fresh) mixtures at 105°C until termination of weight loss. The hydration degree of dry blends was found to be 0.7 ± 0.2 wt%. Dry blends were stored until use over

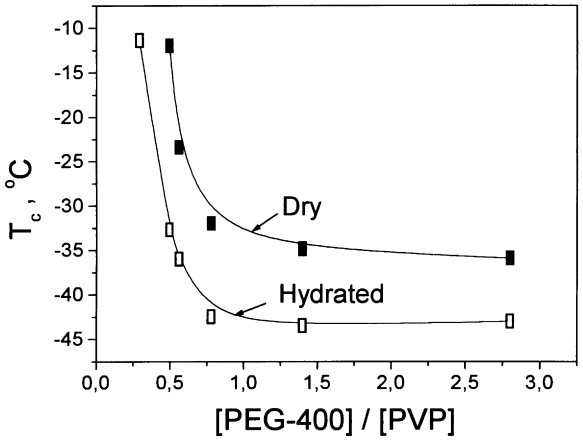

Fig. 2. Dependence of maximum PEG cold crystallization rate temperature, T_c, in freshly prepared (hydrated) and dry PVP–PEG blends on the number of PEG-400 macromolecules available in the blends per PVP unit.

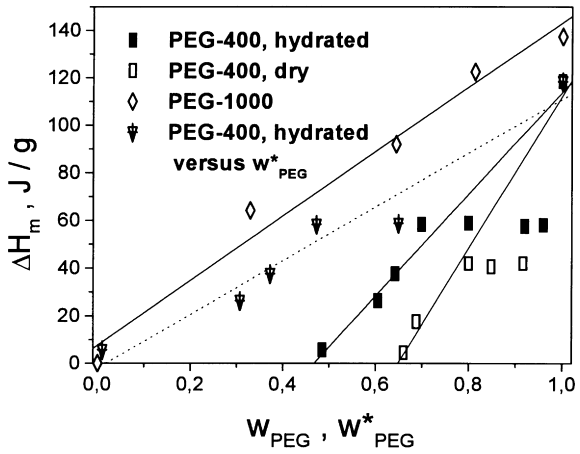

Fig. 3. Heat of fusion, ΔH_m, of freshly prepared (hydrated) and dry PVP blends with PEG-400 and PEG-1000 as a function of PEG weight fraction in the blends, w_{PEG}, and weight fraction of free PEG-400 in blend, w^*_{PEG}.

P_2O_5, while the hydrated blends were exposed to atmosphere humidity at ambient temperature.

Samples were analysed under dry argon in a Mettler TA 4000/DSC 30 DSC thermoanalyser, calibrated with indium and gallium. Samples were cooled with liquid nitrogen in the DSC apparatus from 20 to ∽−150°C over 2–3 min and then heated up to 200°C at a rate of 20°C min^{-1} (unless other program has been noted). T_gs were recorded at half-height of the relevant heat capacity jumps, whereas the T_c and T_m were taken as the temperatures of the cold crystallization and melting peaks. The heats of cold crystallization and melting, determined on the areas of corresponding peaks, were normalised to 1 g of polymer blend. Magnitudes of heat flow in the DSC curves, presented in the figures, are reduced to a reference sample weight of 10 mg.

3. Results and discussion

Fig. 1 shows typical DSC heating curves of PVP, PEG-400 and their blends for the entire range of compositions over the temperature region −100 to 50°C. To elucidate relations between T_c and T_g in greater details we do not consider here the upper temperature range, exhibiting the glass transition of pure PVP and the endotherms of moisture thermodesorption for PVP–PEG blends [14]. The scan of pure PVP displays no thermal events in the region of interest, while for PVP–PEG blends three distinct transitions are discernible. The jump in heat capacity in the region of −70 to −50°C reflects the glass transition. Only a single glass transition is observed which is rapidly shifted to lower temperatures as the PEG content rises. Adding PEG to PVP leads to narrowing of the glass transition and increases the heat capacity change, ΔC_p. The second transition peak between −45 and −11°C is an exotherm, representing PEG cold crystallization in blends. The third is an endotherm around 0–6°C, which is due to PEG melting in the blends. The DSC traces of dry blends have similar character and display the same thermal events, though relevant transition temperatures are somewhat higher. No crystallization and melting processes occur in both hydrated and dry blends at PEG concentrations below 53 wt%, whereas for PEG-rich blends mixing PVP with PEG is accompanied by a rapid drop of the T_c value until a critical PEG concentration of 75 wt% (or 78 PEG-400 molecules per 100 PVP repeat units) is attained, after which the response in the T_c tends to a plateau (Fig. 2). Both the enthalpies of cold crystallization, ΔH_c, and the melting peaks, ΔH_m, are directly proportional to PEG weight fraction in blends, w_{PEG}. As a rule, ΔH_c is always slightly smaller than ΔH_m and the $\Delta H_c/\Delta H_m$ ratio has been found to be 0.88 ± 0.06 for dry and 0.94 ± 0.02 for hydrated blends. The area under the melting endotherm (normalized for sample mass from DSC analysis) is plotted in Fig. 3 as a function of weight fraction of crystalline polymer, PEG. The heats of cold crystallization and melting peaks are reduced by dilution of crystalline PEG with amorphous PVP. No cold crystallization behaviour is observed for PVP-overloaded blends, containing up to 50 wt% PEG-400. Above this point the samples begin to develop 6–12% crystallinity on quench cooling from melt in the DSC apparatus, and consequently the cold crystallization exotherms upon heating become smaller than the corresponding melting endotherms.

The area of the PEG melting endotherm decreases dramatically upon addition of PVP and, as seen in Fig. 3, the blends containing less than 50 wt% of PEG-400 do not develop any crystallinity during thermal cycle employed. The single T_g for these blends and the suppression of PEG cold crystallization caused by PVP provide positive evidence that this system forms a miscible amorphous phase. Further discussion of the data presented in Fig. 3 is given in following sections of this paper.

At first glance it is curious that the liquid PEG-400 freezes in blends not upon cooling from the melt but upon heating quenched samples through their T_gs. As a mixture of

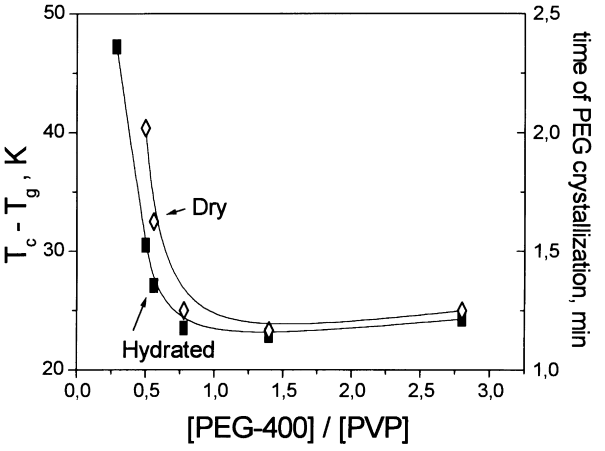

Fig. 4. Composition dependence of the temperature-time range between glass transition and cold crystallization peak for freshly prepared (hydrated) and dry PVP blends with PEG-400.

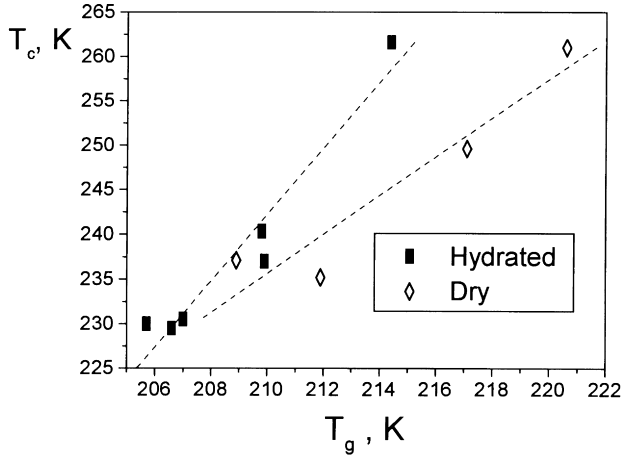

Fig. 5. The PEG maximum cold crystallization rate temperature, T_c, plotted versus glass transition temperature, T_g, of freshly prepared (hydrated) and dry PVP–PEG blends.

amorphous and crystalline polymers is cooled rapidly through its T_g from the melt, the frozen molecular mobility, which maintains it in conformational and phase equilibrium, can no longer occur on the time scale of the cooling process and the material becomes a thermodynamically unstable glass. In this state, no crystallization processes are allowed. PEG crystallization can therefore occur only above the respective T_g, somewhere between T_g and T_m, and this process is referred to as cold crystallization. The growth rate of the crystalline phase depends on the diffusion distance and, consequently, on the concentration of crystallising PEG, randomly distributed within the amorphous phase formed by PVP. Quench-cooled samples of pure PEG are still capable of crystallising at a sufficiently rapid rate during the quenching process to produce a material containing an extensive amount of crystallinity. Therefore, the heating thermogram of pure PEG-400 in Fig. 1 exhibits no cold crystallization exotherm, but does display an endotherm of fusion.

At fixed rate of sample heating above T_g, the T_c–T_g interval represents not only the temperature gradient, required to impart molecular mobility necessary to overcome an energetic barrier of PEG crystallization, but concomitantly it characterises the time needed for cold crystallization. As is evident from the data in Fig. 4, the T_c–T_g interval and the time required for PEG cold crystallization climb sharply as the PEG concentration is decreased below eight PEG-400 macromolecules per ten PVP units available in blends. The increase in T_c–T_g interval is thus a result of severe kinetic restrictions placed on the cold crystallization process by the employed thermal procedure. An additional cause of the inability of blends with high amorphous polymer content to crystallize is the growing isolation of the individual chains of the crystalline polymer with increasing amorphous polymer content due to the random placement of different PEG molecules in the homogeneous compatible state and the above restriction on molecular mobility during the crystallization process. At high amorphous polymer concentration the domains of crystalline polymer have been reported [1] to be smaller than the critical nucleus size for crystallization.

As Fig. 5 illustrates, a linear relationship has been found between the temperature of PEG maximum cold crystallization rate, T_c, upon heating from glassy state the samples obtained by quench-cooling from a melt, and the glass transition temperature, T_g.

For hydrated blends:

$$T_c(K) = (3.72 \pm 0.49)\, T_g - (538.17 \pm 101.71) \quad (1)$$

$$R = 0.967,\ p = 0.0016$$

For dry compositions:

$$T_c(K) = (2.18 \pm 0.51)\, T_g - (222.41 \pm 110.23) \quad (2)$$

$$R = 0.949,\ p = 0.0512.$$

If we accept the concept that the PEG crystallization behaviour in compatible blends with PVP is determined by an activation energy [19], then we must in turn consider those polymer properties that relates to the activation energy, e.g. viscosity, free volume and diffusivity. Since various polymers exhibit similar fundamental properties at their own T_gs (e.g. packing density coefficient of 0.667 [20], fractional free volume, f_g, of 0.025 [21], segmental relaxation time of 5 min [22], microviscosity (molecular friction coefficient) $\eta_g = 0.3\ 10^{-12}\ Pa\ s$ [22], and self-diffusion coefficient of polymer segment $D_g \approx 10^{-21}\ m^2\ s^{-1}$ [23], the T_g values can be taken as the important predictive indicator of polymer behaviour in the operating temperature range $T_g < T < T_g + 150$ K. For the PVP–PEG system under consideration, the T_g value can be therefore used to estimate the variety of viscoelastic and transport properties at maximum crystallization rate temperature, T_c. To give a temperature dependence for η and f, and evaluate these quantities at T_c, the Williams, Landel, Ferry (WLF) and

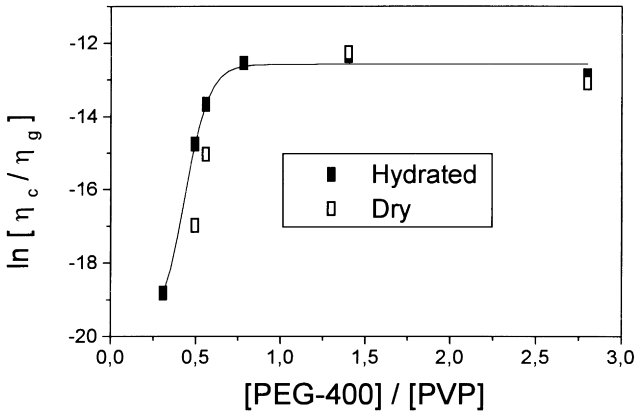

Fig. 6. The plot of the logarithm of apparent microviscosities ratio at T_c and T_g against the composition of dry and hydrated PVP–PEG blends.

the Doolittle equations are appropriate [21]:

$$\ln \frac{\eta_c}{\eta_g} = \frac{1}{f_c} - \frac{1}{f_g} = -\frac{Nf_{cr}}{f_g} \frac{T_c - T_g}{[f_g/\Delta\alpha] + T_c - T_g}$$
$$= -\frac{40.00[T_c - T_g]}{52.08 + T_c - T_g} \quad (3)$$

where η_c, η_g—apparent polymer microviscosities at T_c and T_g respectively; f_c, f_g and f_{cr}—fractional free volume at T_c and T_g as well as a critical fraction of free volume required so that a segment may jump or move; N—the number of moving polymer units per segment, and $\Delta\alpha$—the change of polymer thermal expansion coefficient at T_g. For the majority of polymers [21] $Nf_{cr} \approx 1$, $f_g \approx 0.025$ and $\Delta\alpha \approx 4.8\ 10^{-4}\ K^{-1}$. Substitution of all these constants into Eq. (3) gives an expression ready to use.

Based on the compositional behaviour of T_g in PVP–PEG blends, shown in the first paper in this series [14; Figs. 2 and 3], the apparent microviscosity and fractional free volume were calculated using Eq. (3) for the temperature of PEG

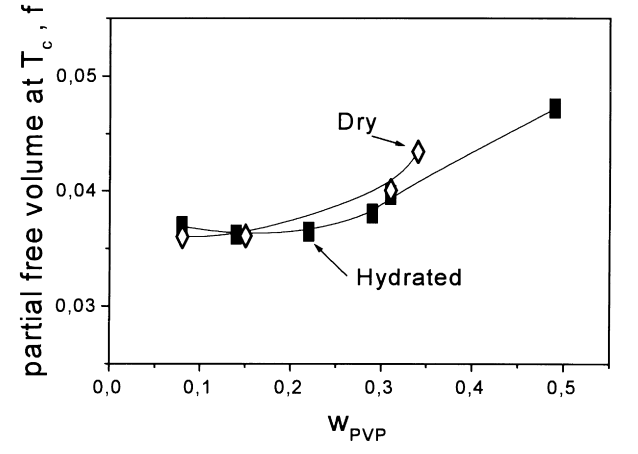

Fig. 7. The plot of partial free volume, f_c, at PEG maximum crystallization rate temperature, T_c, against PVP weight fraction in freshly prepared and hydrated blends.

maximum cold crystallization rate, T_c. The self-diffusion coefficient of polymer segments at T_c (D_c), referred to that at glass transition (D_g), is given by the WLF equation in the form [24]:

$$\log \frac{D_c}{D_g} = \frac{Nf_{cr}}{2.303f_g}\left[1 + \frac{f_g}{\Delta\alpha(T_c - T_g)}\right]^{-1}$$
$$= 17.37\left[1 + \frac{52.08}{T_c - T_g}\right]^{-1} \quad (4)$$

Finally, a free activation energy for polymer crystallization, i.e. an activation energy for PEG chain diffusion through the crystal–melt interface to join growing crystal, ΔG_D, can be estimated from the T_g and T_c values using following the WLF equation [25]:

$$\frac{\Delta G_D}{kT_c} = \frac{2.07 \times 10^3}{51.6 + T_c - T_g} \quad (5)$$

where k is the Boltzmann constant.

The quantities, evaluated from the T_c and T_g with Eqs. (3)–(5), are related to the composition of PVP–PEG compatible blends in Figs. 6–9. Since the microviscosity and self-diffusion coefficient characterise, in essence, the segmental mobility of individual polymer chains but are applied here to describe the mixture of polymers, η and D are to be treated respectively as an apparent microviscosity and an apparent self-diffusion coefficient. The compositional behaviours of these quantities, shown in Figs. 6–9, match closely the composition dependence of T_c and the T_c–T_g interval, presented in Figs. 2 and 4. Two distinct regions are discernible in all the plots. In PVP-underloaded blends ($w_{PVP} \leq 0.24$, or, what is the same, [PEG-400]/[PVP] ≥ 0.78), crystallization occurs at T_c, T_c–T_g, $\log[\eta_c/\eta_g]$, f, $\log[D_c/D_g]$ and at ΔG_D magnitudes which are nearly invariant with composition. This region is therefore thought to embed a thermodynamic equilibrium between T_c and T_g, at which a contribution of the above mentioned kinetic restriction to the cold crystallization process becomes negligible. At equilibrium the T_c/T_g ratio is found to range normally between 1.11 and 1.12, the apparent blend microviscosity is about 5.6 orders of magnitude less than that at T_g, $f_c \approx 0.037$, the D_c is approximately 500,000 times higher than D_g, and $\Delta G_D \approx 52 - 54\ kJ\ mol^{-1}$. In contrast, for the PVP-overloaded blends (at $w_{PVP} > 0.25$ and [PEG-400]/[*PVP*] < 0.7) the T_c/T_g ratio has been found to increase appreciably, approaching the values of 1.22–1.23 (see Fig. 8 in the first paper of this series [14]), and all the quantities provided by Eqs. (3)–(5) are the explicit functions of blend composition (Figs. 6–9). In this composition region PEG cold crystallization proceeds at a substantially decreased apparent microviscosity and activation energy, but at increased free volume and diffusion coefficient, implying that enhanced molecular mobility and crystallization rate are required in order to surpass the diluent effect of amorphous PVP.

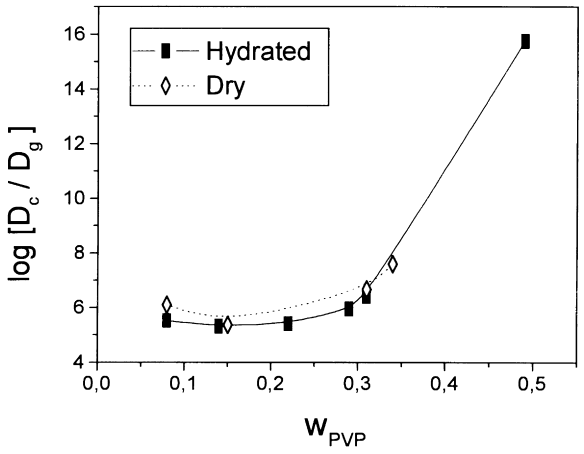

Fig. 8. Effect of PVP concentration (in weight fractions) on apparent polymer self-diffusion coefficient in hydrated and dry PVP–PEG blends at the themperature of maximum cold crystallization rate, D_c, related to the reference value of that at glass transition temperature, D_g.

Crystallization in this region of blend compositions may therefore be characterised as kinetically hindered.

Eq. (5) yields only approximate estimate of ΔG_D. However, the activation energy for PEG crystallization in compatible blends with amorphous PVP, ΔG_c, can be quantified experimentally using the T_c-dependence on the rate of sample heating, ν [26]:

$$\Delta G_c = -R\frac{d(\ln \nu)}{d(1/T_c)} \quad (6)$$

where R is the gas constant.

When the logarithms of scanning rates (10, 20, 30 and 40°C min^{-1}) were plotted against the reciprocals of T_cs, straight lines were obtained with very good fitting, which allowed evaluating the ΔG_c from relevant slopes (Table 1). The obtained data in Fig. 9 and in Table 1 are in very reasonable agreement with those determined with the WLF equation (5). The increase in ΔG_c for PEG-overloaded systems is

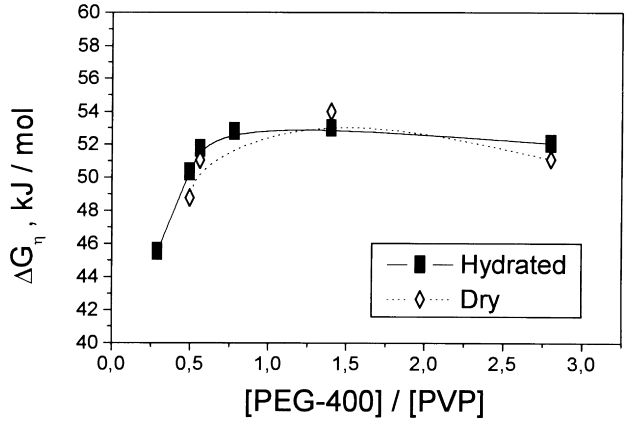

Fig. 9. The composition dependence of viscous flow activation energy for freshly prepared and dry PVP blends with PEG-400 at maximum cold crystallization rate temperature, T_c.

Table 1
Effect of PVP concentration on the activation energy for PEG cold crystallization, ΔG_c, upon heating of the blends, quench-cooled from melt, through their glass transition temperature

Composition		ΔG_c (kJ mol^{-1})	R	p
w_{PVP}	[PEG-400]/[PVP]			
0.34	0.50	59.5 ± 9.5	0.973	0.027
0.31	0.56	63.8 ± 4.3	0.995	0.005
0.24	0.78	56.2 ± 12.2	0.956	0.044
0.15	1.4	90.5 ± 29.1	0.911	0.089
0.08	2.8	96.5 ± 12.6	0.983	0.017

most likely caused by the lack of free PEG available for crystallization, as is shown below. Since PEG cold crystallization in the blends with amorphous PVP involves a diffusion process, it is of interest also to compare the ΔG_D and ΔG_c values with an activation energy for PVP–PEG interdiffusion, measured by an optical microinterference technique [27], that has been found to increase from 30 to 39 kJ mol^{-1} as PVP weight fraction increases from 0.1 to 0.5.

Diffusion seems to take a considerable portion of the activation energy required for PEG cold crystallization. The ΔG_D and ΔG_c magnitudes in Fig. 9 and in Table 1 are close to the value of apparent activation energy for viscous flow, ΔG_η, measured with a squeezing flow technique [28] from the temperature dependence of PVP–PEG blend shear viscosity and found to be $\Delta G_\eta \approx 54$ kJ mol^{-1} for the blend containing 36 wt% PEG-400.

It is worthy of note that the activation energy of crystalline polymer chain diffusion through the crystal–melt interface, ΔG_D, shown in Fig. 9 as a function of PVP–PEG blend composition, is in essence identical to the ΔE parameter [14], introduced by Okui [19] and defined as an activation energy for migration of polymer segment through the nucleus–melt interface. However, notwithstanding the fact that ΔG_D reveals the drop with PEG content decrease (Fig. 9), the $\Delta E/K$ quantity in the first paper of this series [14; Fig. 13] displays evident growth with reduction in PEG concentration. These seemingly inconsistent findings can be easily reconciled by the plausible conjecture that the nucleation parameter K, defined in [14] by Eqs. (11), rises dramatically with increase in amorphous PEG content. Indeed, by definition K is inversely related to the heat of fusion, ΔH_m, which approaches zero rapidly with amorphous PVP addition to crystalline PEG (Fig. 3). The PVP is generally recognised as an inhibitor of crystallization [29] and the observed effects in the compositional behaviour of the ΔG_D and $\Delta E/K$ quantities in PVP–PEG blends serve as example of its anti-nucleation activity.

According to Okui [19] and our results (Figs. 6–9) the T_c–T_g relationship in Fig. 5 invokes PEG molecular mobility, expressed in the terms of the activation energy. This inference can be derived more explicitly from the following simple physical reasoning. The logarithm of the ratio

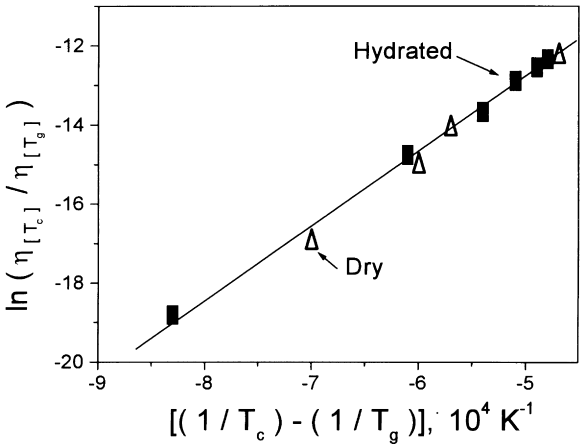

Fig. 10. The Frenkel–Eyring plot of blend apparent microviscosities ratio at maximum PEG cold crystallization rate temperature, T_c, and the temperature of blend glass transition, T_g, against the difference of reciprocals these temperatures.

between polymer blend apparent microviscosities at T_c and T_g, calculated using the WLF equation (3) and presented as a function of blend composition in Fig. 6, yields a straight line when is plotted against the difference of reciprocals of these temperatures (Fig. 10).

For hydrated compositions:

$$\ln \frac{\eta_c}{\eta_g} = 18381.88\left[\frac{1}{T_c} - \frac{1}{T_g}\right] - 3.58 \tag{7}$$

$R = 0.999;\ \ p < 0.0001$

For dry blends:

$$\ln \frac{\eta_c}{\eta_g} = 20611.30\left[\frac{1}{T_c} - \frac{1}{T_g}\right] - 2.54 \tag{8}$$

$R = 0.997;\ \ p = 0.0025$

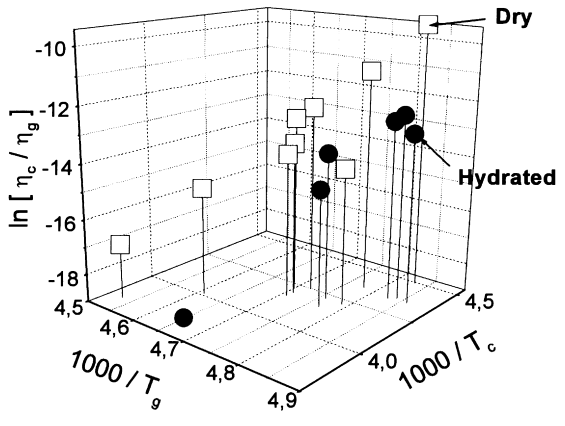

Fig. 11. Three-dimensional plot of the logarithm of blend microviscosities ratio at maximum PEG cold crystallization rate temperature, T_c, and the temperature of blend glass transition, T_g, against the reciprocals these temperatures.

According to the Frenkel–Eyring's activation theory [30] at $T > T_g$:

$$\eta = \frac{N_a h}{V}\, e^{\Delta G_\eta / RT} \tag{9}$$

where N_a is Avogadro's number, h is Planck's constant, V is the molecular volume of moving polymer segment and ΔG_η is the activation energy for viscous flow. Substituting Eq. (9) into Eq. (3) and considering that $\Delta G_\eta = \Delta H_\eta - T\Delta S_\eta$ gives:

$$\ln \frac{\eta_c}{\eta_g} = \frac{(\Delta S_\eta)_g - (\Delta S_\eta)_c}{R} + \frac{(\Delta H_\eta)_c}{RT_c} - \frac{(\Delta H_\eta)_g}{RT_g} \tag{10}$$

where ΔH_η is the enthalpy and ΔS_η, the entropy of activation for viscous flow.

The multiple linear regression of the $\ln(\eta_c/\eta_g)$ quantity on two variables, $1/T_c$ and $1/T_g$ (Fig. 11) allows estimating the changes in the activation enthalpies of viscous flow at T_c and T_g, respectively, as well as the difference between activation entropies at these temperatures. For hydrated blends we have:

$$\ln \frac{\eta_c}{\eta_g} = -18.2 + \frac{16894.3}{T_c} - \frac{14017.4}{T_g}, \quad R^2 = 0.999 \tag{11}$$

$(\Delta S_\eta)_g - (\Delta S_\eta)_c = -151\ \text{J mol}^{-1}$;

$(\Delta H_\eta)_c = 140.4\ \text{kJ mol}^{-1}$;

$(\Delta H_\eta)_g = 116.5\ \text{kJ mol}^{-1}$.

For dry blends:

$$\ln \frac{\eta_c}{\eta_g} = -12.6 + \frac{19457.9}{T_c} - \frac{17448.3}{T_g}, \quad R^2 = 0.996 \tag{12}$$

$(\Delta S_\eta)_g - (\Delta S_\eta)_c = -105\ \text{J mol}^{-1}$;

$(\Delta H_\eta)_c = 161.7\ \text{kJ mol}^{-1}$;

$(\Delta H_\eta)_g = 145.0\ \text{kJ mol}^{-1}$.

With respect to drawing on the WLF equation to help understand the rational behind the T_c–T_g relationship, a range of reservations should be here stated. First, it may appear that the analysis presented by the Eqs. (7), (8), (10) and (12) and Figs. 9 and 10 is somewhat irrelevant because the $\ln(\eta_c/\eta_g)$ quantity is plotted against the same variables T_c and T_g, from which it has been calculated. However, since according to Eq. (3) the numerical magnitude of this quantity is determined solely by the T_g and T_c values, and both these variables are measured independently from DSC traces, this procedure enables us to treat the expressions for $\ln(\eta_c/\eta_g)$, $\ln(D_c/D_g)$, f_c and ΔG_D, provided by the Eqs. (3)–(5), as specific forms of the T_c–T_g relationship shown in Fig. 5, which demonstrates a clear physical

Table 2
The hypothetic maximum cold crystallization rate temperature for PEG-400 within PVP-overloaded blends, evaluated with Eqs. (1), (2), (7) and (8)

PEG content (wt%)	Hydration degree (wt%)	Measured T_g (°C)	Calculated T_c (°C)	Equation no.
36	1.3	−32.5	28.9	(2)
			21.9	(8)
	8.4	−53.1	5.8	(1)
			−0.7	(7)
50	0.3	−50.5	−10.3	(2)
			−2.3	(8)

meaning. In this connection the analysis of the T_c and T_g contributions to any of this quantities seems to be quite pertinent. The same treatment may be applied equally well to the $\ln(D_c/D_g)$ quantity, eliciting the apparent activation energy for diffusion as a factor controlling the T_c–T_g relationship instead of the activation energy for viscous flow.

The second reservation relates to the significance of ΔH_η and ΔS_η magnitudes obtained with the multiple linear regression. Since the T_c and T_g are mutually dependent variables, as is established unequivocally by the data in Fig. 5, the results of regression are fitted coefficients rather than the true activation enthalpies and entropies for viscous flow at T_g and T_c. Nevertheless, the employed approach provides a qualitative insight into the mechanism by which the T_c is controlled by the T_g in PVP–PEG compatible blends.

The Eqs. (1), (2), (7) and (8) have been employed to explain why no PEG cold crystallization occurs within PVP-overloaded blends (at PEG concentration $w_{PEG} < 0.5$, Figs. 1 and 3). Using the T_g values derived from the DSC thermograms of the PVP-overloaded blends, we have calculated the expected PEG maximum cold crystallization temperatures, which have been found to exceed appreciably the onset temperature of pure PEG-400 melting (−23°C) and even the temperature of PEG fusion peak (6°C). The data are listed in Table 2, indicating that PEG cold crystallization is not allowed at $w_{PEG} \leq 0.5$ due to kinetic restriction. In order to explore whether the kinetic inhibition has been aggravated by PVP–PEG binding we have modified the thermal cycle employed. The blend containing 36 wt% of PEG-400 and demonstrating $T_g = -54$°C was cooled slowly to −40°C at a cooling rate of 2°C min^{-1} and then annealed at this temperature for 1 h. Annealing was followed by further cooling the sample to −150°C with the rate of 5°C min^{-1}. The cooled specimen was then heated up to 200°C in the DSC measuring cell at a heating rate of 20°C min^{-1}. No signs of crystalline phase was detected in the blend after this procedure.

Whilst the lack of cold crystallization–melting phenomena in the PVP-overloaded blends can not be unequivocally indicative of complete PEG binding with the PVP due to kinetic reasons, it does not still argue against such binding. We turn now back to Fig. 3, where the areas under PEG melting endotherms in dry and hydrated blends are plotted against the weight fraction of crystalline PEG. If PVP merely diluted PEG causing kinetic hindrance and did not interfere with its crystallinity through a strong favourable interaction, the plot would represent the straight line connecting the origin ($\Delta H_m = 0$ at $w_{PEG} = 0$) and the heat of fusion of pure PEG-400 ($\Delta H_m = 118$ J g^{-1} at $w_{PEG} = 1$). Such ideal dilution behaviour is in fact typical of the PVP blends with PEG-1000 ($\Delta H_m = 136.6$ J g^{-1}, $T_m = 39$°C) as is illustrated by the data in Fig. 3. In contrast to the phase behaviour of PVP mixtures with PEG-400, no cold crystallization exotherms are detected in DSC heating traces of PVP blends with PEG-1000, quench-cooled both from ambient temperature (20°C) and from the molten state (60°C), and only melting peaks remain to signify the presence of the crystalline phase. Annealing the samples in the melt (60°C for 60 min) prior to their quench cooling in liquid nitrogen does not affect the heats of fusion and crystallinity, whereas appreciable depression in PEG-1000 melting temperature in the annealed blends (e.g. by 5.7°C for the blend containing 16.4 wt% of amorphous PVP) signifies the formation of compatible blends.

Unlike the PVP blends with PEG-1000, the enthalpy of PEG-400 melting in the blends with the same amorphous polymer decreases abruptly with increasing PVP concentration (Fig. 3). The disappearance of the melting peak due to free PEG-400 in PVP, and the reduction in heat of fusion to less than that resulting from simple dilution with amorphous PVP demonstrates that a significant amount of liquid PEG does not freeze in blends over entire composition range. This is presumably due to interaction (binding) of PEG molecules with the PVP. If solely kinetic restriction was the reason for non-freezing PEG-400 in PVP-overloaded blends, all the PEG would be available for crystallization within the PEG-overloaded blends ($w_{PEG} > 0.7$), where cold crystallization has been shown above to be kinetically allowed. However, the lack of equivalence between crystallinity and the total amount of PEG-400 in blends reveals the non-freezing PEG occurrence within a composition range where no kinetic hindrance takes a place. A feasible method of estimating the bound (non-crystallising) PEG is to plot the heat of free PEG fusion per gram of polymer blend versus the total weight of PEG per gram of the blend (w_{PEG}) and extrapolate to zero for the ΔH_m. The PEG binding with PVP obtained in this manner is found to be ∽0.49 and ∽0.63 g PEG-400/g polymer blend, or 0.26 and 0.47 PEG-400 macromolecules per PVP repeat unit respectively

for hydrated and dry mixtures (Fig. 3). In the case of constant PEG binding degree per gram of polymer blend over the concentration range employed, i.e. at $w_{PEG} > 0.5$ for hydrated and 0.65 for dry blends, the relationship should be linear as is in fact seen in Fig. 3. The invariability of the binding degree within a wide composition range in PEG-overloaded blends is evidence for PVP–PEG complex stoichiometry. The stoichiometric composition of the PVP–PEG complex, evaluated on the data in Fig. 3, is in excellent agreement with the results of FTi.r. analysis of hydrogen bonds formed between PEG terminal hydroxyl groups and carbonyls in the PVP repeat units, and matches closely the PVP–PEG binding degree determined from the compositional dependence of the glass transition temperature [16].

If all the PEG-400 were free and available for crystallization in the blends with PVP, the slope of the ΔH_m–w_{PEG} linear plot (Fig. 3) would yield the heat of fusion for pure PEG. This is the case for PVP blends with PEG-1000, but the slopes for PEG-400 compositions with PVP are significantly greater than the theoretical value (246 and 312 J g^{-1} for hydrated and dry blends respectively). By this way the data obtained show no ΔH_m correlation with the total PEG-400 content in a system. In contrast, as the weight fraction of free PEG is used, w^*_{PEG}, defined as the difference between total PEG amount and the weight of bound PEG, the calculated slope exhibits good agreement with the ΔH_m of pure PEG-400 (Fig. 3).

Conceivably the most credible and unambiguous evidence that the non-freezing PEG must be identified as the PEG bound in stoichiometric complex with amorphous PVP, and that the lack of cold crystallization-melting processes within the PVP-overloaded blends is caused eventually by PEG binding which aggravates kinetic restriction imposed upon crystallization, is provided by the fact that in kinetically non-restricted blends ($w_{PEG} \geq 0.8$) the heat of free PEG fusion reaches a fixed limiting value, ΔH^{∞}_m, decreased dramatically compared to that of pure PEG-400. As is seen from Fig. 3, the hydrated PEG-overloaded blends display $\Delta H^{\infty}_m \approx 58$ J g^{-1}, while for dry blends this value is found to be $\Delta H^{\infty}_m \approx 41.5$ J g^{-1}. PEG's inability to be fully crystallized in PVP-underloaded blends is also manifested by increased activation energy for cold crystallization, presented in Table 1. Dividing the ΔH^{∞}_m by the reference value of pure PEG-400 heat of fusion (118 J g^{-1}) yields the weight fraction of free, crystallizable PEG-400, whereas the weight fraction of non-freezing, bound PEG can be determined as a difference between the amounts of total and free PEG in the blends, $1 - (\Delta H^{\infty}_m/\Delta H_{mPEG})$. The PEG binding degree with PVP, evaluated with this procedure, is calculated to be ~0.51 and 0.65 g bound PEG per gram mixture for hydrated and dry systems respectively. These magnitudes are in close agreement with those evaluated earlier from the intercepts of linear plots in Fig. 3 at $\Delta H_m = 0$. The invariability of the ΔH^{∞}_m values with blend composition implies stoichiometry of the PVP–PEG complex.

The area under melting endotherm, ΔH_m, is a measure of blend crystallinity, representing an explicit function of the crystalline polymer content (Fig. 3). From this standpoint the ΔH_m is thought to be independent on the rate of heating. This is really the case for pure PEG, however for the PEG blends with amorphous PVP the ΔH_m decreases linearly with the rate of heating as displayed by the data in the Table 1 of the previous work [14]. This is a result of kinetic hindrance in PEG cold crystallization process that is aggravated with the increase in heating rate as is embedded by the concomitant reduction in ΔH_c.

4. Conclusions

The cold crystallization of free PEG-400 in compatible blends with amorphous PVP occurs upon heating through glass transition the samples prepared by quench-cooling from the melt. Under the thermal cycle employed the peak temperature of cold crystallization exotherm, T_c, has been found to represent an explicit function of T_g and blend composition. The examination of the T_c dependence on T_g with respect to the PVP concentration, performed in the terms of apparent polymer microviscosity and diffusivity as well as fractional free volume at T_c, reveals relevant activation energies, in particular the activation energies for viscous flow or diffusion, as factors controlling the T_c. As the PEG content in blends increases, the contribution of kinetic restriction to the temperature of PEG maximum cold crystallization rate becomes negligible. The amount of non-freezing PEG is determined from the decrease in heat of fusion of PEG-400 at various PVP concentrations in blends. The disappearance of any PEG crystallization and melting processes within PVP-overloaded blends has been shown to be caused by the amorphous polymer diluent effect resulting in kinetic hindrance. In contrast, the occurrence of non-crystallizable PEG within kinetically non-restricted PVP-underloaded systems relates unambiguously to a strong favourable PVP–PEG interaction and stoichiometric complex formation. The stoichiometry of PVP–PEG complex has been established from DSC thermograms as the amount of PEG unavailable for crystallization, which has been demonstrated to be invariable with composition in the PEG-overloaded blends.

Acknowledgements

This research was, in part, made possible by Award No. RN2-409 of the US Civilian Research and Development Foundation for the Independent States of the Former Soviet Union (CRDF). We express our appreciation to Academician Nicolai A. Platé, Professor Ronald A. Siegel, and Professor Anatoly E. Chalykh, for their helpful discussion and comments.

References

[1] MacKnight WJ, Karasz FE, Fried JR. In: Paul DR, Newman S, editors. Polymer blends, 1. New York: Academic Press, 1978 chap. 5.

[2] Nishi T, Wang TT. Melting point depression and kinetic effects of cooling on crystallization in poly(vinylidene fluoride)–poly(methyl methacrylate) mixtures. Macromolecules 1975;8(6):909–15.

[3] Ma CCM, Wu HD, Lee CT. Strength of hydrogen bonding in the Novolak-type phenolic resin blends. J Polym Sci Polym Phys 1998;36:1721–9.

[4] Cruz CA, Barlow JW, Paul DR. Polyester–polycarconate blends. VII. Ring-containing polymers. J Appl Polym Sci 1980;25:1559–71.

[5] Pompe G, Haubler L, Winter W. Investigations of the equilibrium melting temperature in PBT and PC/PBT blends. J Polym Sci Polym Phys Ed 1996;34:211–9.

[6] Rostami S. Crystallization behaviour of a semicrystalline miscible blends. Polymer 1990;31(5):899–904.

[7] Kalfoglou NK. Compatibility of poly(ethylene oxide)–poly(vinyl acetate) blends. J Polym Sci Polym Phys Ed 1982;20:1259–67.

[8] Walsh DJ, Singh VB. The phase behaviour of a poly(ether sulfone) with poly(ethylene oxide). Makromol Chem 1984;185:1979–89.

[9] Morra BS, Stein RS. Melting studies of poly(vinylidene fluoride) and its blends with poly(methyl methacrylate). J Polym Sci Polym Phys Ed 1982;20:2243–59.

[10] Quintana JR, Cesteros LC, Peleteiro MC, Katime I. Study of the melting and crystallization behaviour of poly(ethylene oxide)–poly-(vinyl alchohol) blends. Polymer 1991;32(15):2793–8.

[11] Silva MA, De Paoli M-A, Felisberti MJ. Flory–Huggins interaction parameter of poly(ethylene oxide)/poly(epichlorohydrin) and poly-(ethylene oxide)/poly(epichlorohydrin-*co*-ethylene oxide) blends. Polymer 1998;39(12):2551–6.

[12] Cesteros LC, Quintana JR, Fernandez JA, Katime I. Miscibility of poly(ethylene oxide) with poly(*N*-vinyl pyrrolidone): DMTA and DTA studies. J Polym Sci Polym Phys Ed 1989;27:2567–76.

[13] Mohn RN, Paul DR, Barlow JW, Cruz CA. Polyester–polycarbonate blends III. Polyesters based on 1,4-cyclohexanedimethanol/terephthalic acid/isophthalic acid. J Appl Polym Sci 1979;23:575–87.

[14] Feldstein MM, Shandryuk GA, Kuptsov SA, Platé NA. Coherence of thermal transitions in poly(*N*-vinyl pyrrolidone)–poly(ethylene glycol) compatible blends. 1. Interrelations among temperatures of melting, maximum cold crystallization rate and glass transition. Polymer 2000;41:5327–38.

[15] Feldstein MM, Lebedeva TL, Shandryuk GA, Kotomin SV, Kuptsov SA, Igonin VE, Grokhovskaya TE, Kulichikhin VG. Complex formation in poly(*N*-vinyl pyrrolidone–poly(ethylene glycol) blends. Polym Sci 1999;41(8):854–66.

[16] Feldstein MM, Lebedeva TL, Shandryuk GA, Igonin VE, Avdeev NN, Kulichikhin VG. Stoichiometry of poly(*N*-vinyl pyrrolidone)–poly(ethylene glycol) complex. Polym Sci 1999;41(8):867–75.

[17] Feldstein MM, Lebedeva TL, Igonin VE, Platé NA. The varieties of poly(ethylene glycol) state in H-complex with poly(*N*-vinyl pyrrolidone). Proceedings International Symposium Control Release Bioactive Materials, 25. , 1998. p. 850–1.

[18] Feldstein MM, Shandryuk GA. Quantitative relation of glass transition temperature to polymer–plasticizer binding degree. Proceedings Internnational Symposium on Controlled Release of Bioactive Materials, 26. , 1999. p. 1084–5.

[19] Okui N. Relationships between melting temperature, maximum crystallization temperature and glass transition temperature. Polymer 1990;31(1):92–4.

[20] Askadsky AL, Matveev YuI. Chemical structure and physical properties of polymers, Moscow: Chemistry, 1983 p. 24–48.

[21] Ferry JD. Viscoelastic properties of polymers, 2. New York: Wiley, 1970 chap. 11.

[22] Bartenev GM, Barteneva AG. Relaxation properties of polymers, Moscow: Chemistry, 1992 p. 138.

[23] Lee L-H. Recent studies in polymer adhesion mechanisms. In: Lee L-H, editor. Adhesive bonding, London: Plenum Press, 1991. p. 1–30.

[24] Fujita H. Diffusion in polymer–diluent systems. Fortsch Hoch Polym 1961;3:1–47.

[25] Wunderlich B. chap. 1. Crystal nucleation, growing, annealing, Macromolecular physics, 2. London: Academic Press, 1978.

[26] Bershtein VA, Egorov VM. Differential scanning calorimetry of polymers, New York: Horwood, 1994 chap. 2.

[27] Igonin VE, Avdeev NN, Feldstein MM. Peculiarities of poly(*N*-vinyl pyrrolidone dissolution in liquid poly(ethelene glycol). Polym Sci 2000;42.

[28] Kotomin SV, Borodulina TA, Feldstein MM, Kulichikhin VG. Sqeeze–recoil analysis of adhesive hydrogels and elastomers. Polym Mater Sci Engng 1999;81:425–6.

[29] Kirsh YE. Water soluble poly(*N*-vinylamides), New York: Wiley, 1998 chap. 4.

[30] Tager AA. Physicochemistry of polymers, 3. Moscow: Mir, 1978 chap. 10.